Olsen, P.E. & Whiteside, J.H, p. 826-835.

ENCYCLOPEDIA OF EARTH SCIENCES SERIES

ENCYCLOPEDIA *of* PALEOCLIMATOLOGY AND ANCIENT ENVIRONMENTS

edited by

VIVIEN GORNITZ
Goddard Institute for Space Studies
and
Columbia University
New York
USA

Springer

2008
ISBN: 978-1-4020-4551-6

PRE-QUATERNARY MILANKOVITCH CYCLES AND CLIMATE VARIABILITY

Introduction

Cyclic variations in insolation, caused by the precession and obliquity of Earth's spin axis and variations in the eccentricity of Earth's orbit, have been stressed as a driver of Quaternary climate since Hays et al. (1976). The Quaternary, however, comprises only 0.4% of Earth history, and is characterized by unusual "ice house" conditions. In addition, neither the mechanism through which ice house conditions were initiated, nor the mechanism whereby the 100 kyr cycle has come to dominate glacial oscillations are understood (see Muller and MacDonald, 2000). Analysis of pre-Quaternary Milankovitch cycles provides a more synoptic view of the role of astronomically controlled climate change, a context for understanding the present state of the Earth system and anthropogenic modifications, a mechanism for producing high-resolution timescales, and data for calibrating the dynamic evolution of the solar system (see reviews by Berger et al., 1989; Fischer et al., 1991; Schwarzacher, 1993; Weedon, 1993, 2003; Hinnov, 2000, 2005).

Methods

Two fundamentally different, although mutually illuminating, approaches to the analysis of pre-Quaternary Milankovitch cyclicity have been developed. The first, cycle counting, predates acceptance of the Milankovitch theory for Quaternary climate change by nearly a century (e.g., Gilbert, 1895) (Figure P88). Cycle counting is an inherently typological approach requiring both identification of each sedimentary or proxy cycle and its boundaries within a section and a timescale to determine cycle duration. Bundles of cycles of variable thickness allow recognition of the characteristic Milankovitch cycle hierarchy based on the thickness ratio of short to long cycles, assuming the highest frequency cycles have been correctly identified. A variant of the cycle counting approach is named for Fischer's (1964) analysis of the Triassic asymmetric carbonate Lofer cycles (Figure P89). These so-called Fischer plots are graphs of cumulative departure from average cycle thickness plotted against cycle number, assuming a uniform period for each cycle and modified for assumed constant subsidence during each cycle (see Sadler et al., 1993; Boss and Rasmussen, 1995 for criticism). While the typological cycle counting method allows easy visualization of sedimentological patterns and cycle identification in the field, the numerous ad hoc assumptions that must be made about the variability of the cyclicity makes its practical use treacherous unless there is a known target pattern for correlation, such as an age-appropriate and accurate insolation curve. Additionally, often used as a measure of relative sea-level change, Fischer plots appear to be a poor predictor for Quaternary examples where sea-level change is well understood (e.g., Boss and Rasmussen, 1995).

The second approach, time series analysis, is commonly used in Quaternary analyses and was inspired by the pivotal paper by Hays et al. (1976) that established Milankovitch cyclicity as the "Pacemaker of the Ice Ages," although there were earlier applications. Here, a variable (lithological or climate proxy) is plotted against thickness or time, and Fourier or other quantitative methods are used to determine the frequency properties of the data that can then be compared to a hypothesis of orbital forcing (Figure P90). This method dispenses with the need to identify the cycle type, has the advantage of not requiring variability in the data to be discarded, and thus does not presume the mode of cyclicity (i.e., precession vs. obliquity). The disadvantage is that the variable must have a unimodal relationship to climate or a precise timescale must be available; these become progressively much less common in more ancient deposits. Sequences have typically been analyzed by Fourier methods with the data transformed from the depth or time domain to the frequency domain. The results are usually expressed as a periodogram (a graph of frequency against a measure of the importance of that frequency, such as power). This method, however, presumes little variation in accumulation rate; that is, the frequencies are stationary with respect to the depth scale. This assumption can be considerably relaxed with use of evolutive or depth-frequency analysis. Here, the frequency properties of the section are analyzed by use of a moving window and are plotted with respect to depth (Figure P91). A plethora of techniques is available in which accumulation rate changes can be determined directly from the internal frequency properties of the data.

Timescales

Both cycle counting and time series methods require a timescale to help assess accumulation rates. Accumulation rates are quantified by relying largely on direct dating by annual rhythms (varves) and radiometric methods, indirect dating by correlation to other well established timescales, such as $\delta^{18}O$ curves or magnetic polarity transitions, and tuning to insolation curves based on celestial mechanics. In older stratigraphic

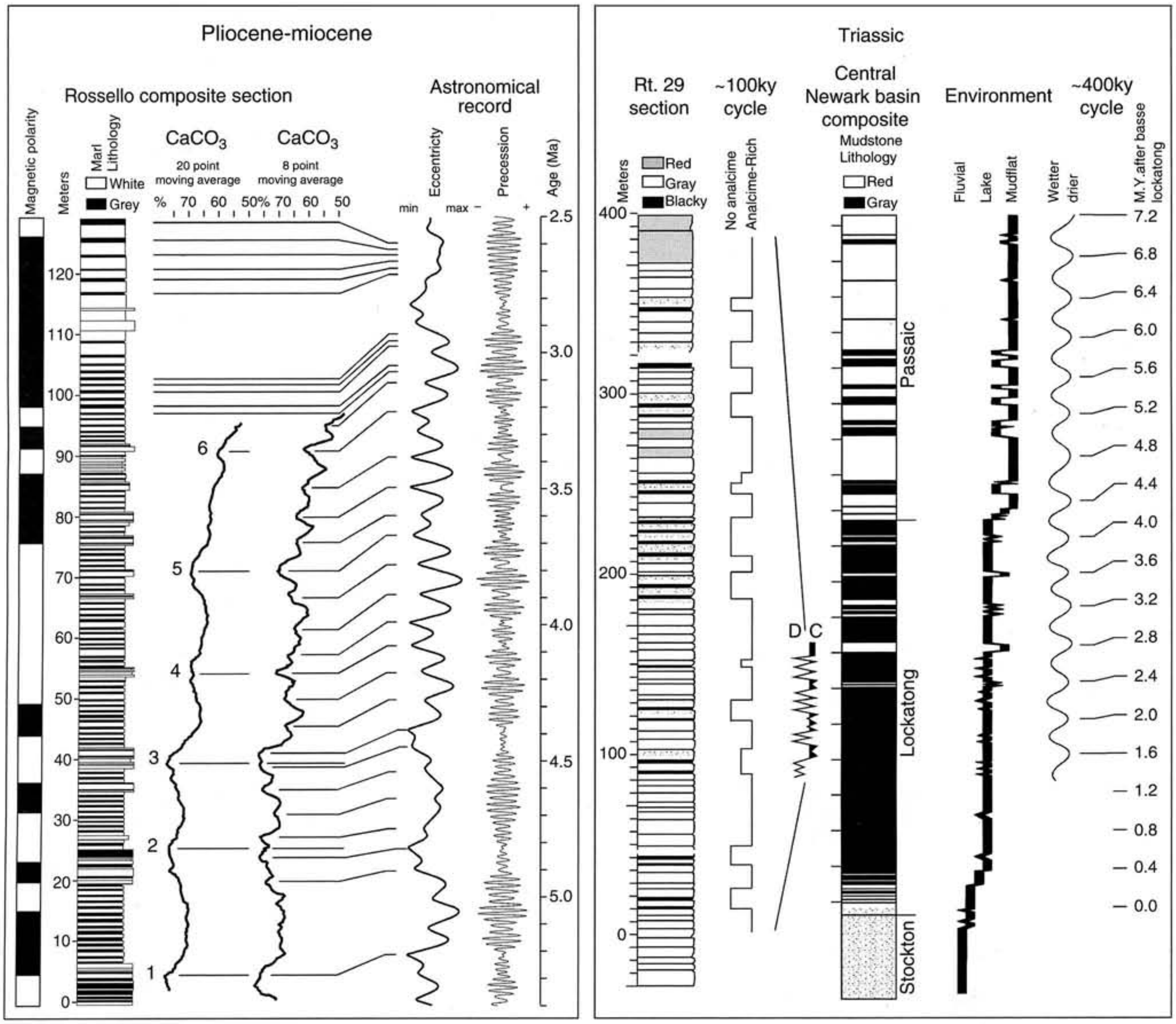

Figure P88 Cycle counting and matching to an astronomical record; *left*: marine Pliocene-Miocene example with astronomical calibration from Sicily modified from Hilgen (1991b); *right*: lacustrine Triassic example, modified from Van Houten (1964) with 400 kyr cycle added.

records, it becomes progressively harder to apply these proxies and dating methods successfully and other, more inferential, methods must be used.

Varves are annual rhythms that can be marine or non-marine and generally consist of couplets or, more rarely, of triplets of heterogeneous laminae (see review by Anderson, 1964; Anderson and Dean, 1988). It is usually assumed that a single couplet or lamina series represents one year, corresponding to summer and winter or wet and dry seasons, although some lacustrine environments could theoretically possess two couplets of laminae series per year, and there can be confusion with tidal banding. Although varve calibration provides direct and very high-resolution records of accumulation rates, varved sequences are rare and when present often constitute only a small part of the sedimentary column.

Radiometric dates provide another direct way to calibrate accumulation rates and a basis for a timescale. To be useful, there must be several dates in a section separated in time sufficiently to exceed error limits, and they must be geologically accurate. Very few sections meet these criteria. It is possible to obtain paleontological or other time-correlative means to tie radiometric dates to sections under analysis. Possible difficulties are exemplified by debates on the Triassic Latemar and the Eocene Green River Formation (Hinnov and Goldhammer, 1991; Brack et al., 1996; Pietras et al., 2003; Machlus et al., 2004, 2008).

As is true for Quaternary records, the relatively well-established marine $\delta^{18}O$ record provides a powerful tie to published timescales for older Neogene marine sections (e.g., Miller et al., 1987). The temporal accuracy, however, of correlations to the

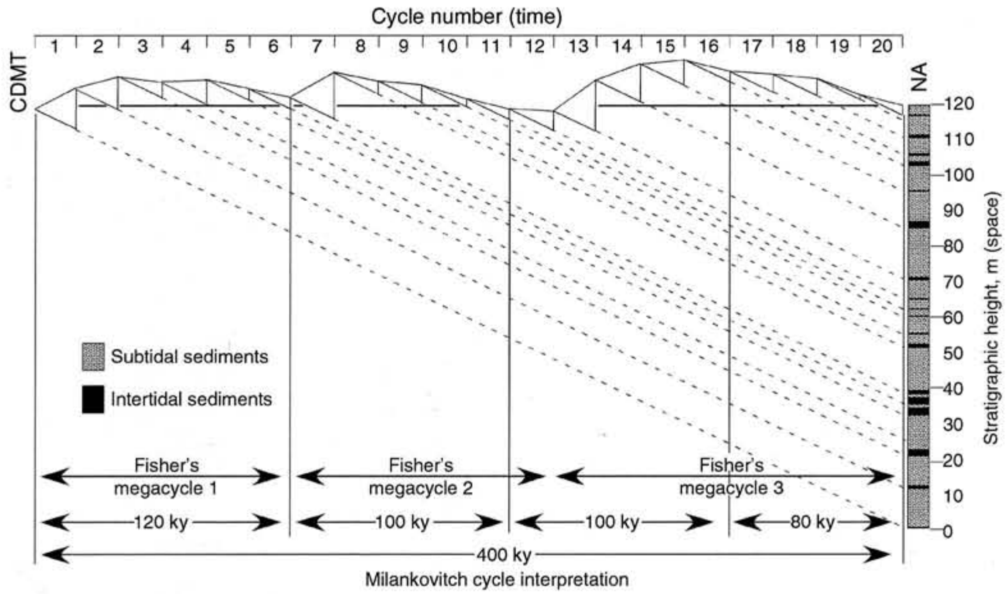

Figure P89 Fischer plot of Fischer's example of Triassic Lofer cycles in marine Triassic carbonates of Austria (modified from Fischer, 1964) with a modern Milankovitch cycle interpretation overlain.

$\delta^{18}O$ record can be no better than the accuracy of the $\delta^{18}O$ record itself, which is undergoing significant modifications. Using this technique for accumulation rate calibration, only open marine sections can be meaningfully correlated, and the section being correlated needs sufficient temporal scope to encompass enough of the character of the $\delta^{18}O$ curve.

Correlation and tuning to insolation curves has been extensively used in strata of Neogene age, but less commonly in the Paleogene (e.g., Hilgen, 1991a,b; Shackleton et al., 2000), and not at all in the Mesozoic and older strata (Figure P88). The production of insolation curves to which ancient proxy curves can be matched is limited by uncertainties in observations, chaotic behavior of the planets, lack of knowledge of the evolution of the Earth-Moon system, and dynamic aspects of mass distribution within the Earth. Insolation curves for the higher frequency climatic precession and obliquity cycles are accurate to 40–50 Ma, and the 405 kyr cycle to 250 Ma. The variations of the 405 kyr cycle beyond 250 Ma are relatively small, and could be used, recognizing the larger uncertainties, back to the age of the Earth (see Laskar, 1990, 1999; Berger et al., 1992; Laskar et al., 1993, 2004; Palike et al., 2004). If the 405 kyr cycle can be identified, it can be used to calibrate average accumulation rate and hence provide a mechanism to establish the period of higher frequency cycles independent of their drift through deep time (e.g., Olsen and Kent, 1999).

For the late Jurassic through Neogene, the well-established marine magnetic anomaly timescale (Cande and Kent, 1995) establishes broad constraints for sections with internal polarity data. Although the average duration of a chron is ~0.25 million years (Lowrie and Kent, 2004), correlation to the marine magnetic anomaly timescale is useful only for sections involving millions of years. As there is no marine magnetic anomaly timescale for strata older than late Jurassic, Milankovitch cycles have proved more useful for calibrating the magnetic polarity record than vice versa (e.g., Kent and Olsen, 1999).

One of the most powerful methods of calibrating accumulation rate is via the internal frequency structure of the data series itself, and this takes two basic forms. First, the celestial mechanical theory predicts a very specific relationship between the higher and lower frequencies present in data. The lower frequencies are beat cycles of the higher frequencies within the precession-related bands or the obliquity-related bands. The frequencies of the ~100 kyr eccentricity cycles are equal to the differences between the frequencies of the climatic precession cycles because these cycles result from the interaction of the Earth's precession and the gravitational attraction of the planets and the eccentricity cycles result from the gravitational interaction of the very same planets. At present, the main periods that can be recognized in climatic precession are about 19, 23, and 24 kyr. The periods of the linear combinations of differences of the frequencies of these periods are about 93, 125, and 405 kyr (calculated using appropriate precision). This is a mathematical relationship that holds regardless of changes in the value of the precession constant in the deep past (due to the Earth-Moon system evolution or mass distribution within the Earth), or chaotic changes in planetary orbits. The same relationship is maintained for the obliquity-related cycles. However, only the most high-fidelity records (e.g., Triassic Lockatong Formation; Olsen and Kent, 1996; Hinnov, 2005) have this level of detail (Figure P89). The second, more widely used concept is that the ratio of the shorter to the longer periods within the Milankovitch bands, such as precession to eccentricity, changes very slowly through Earth history, presently there is a 1:5:20 ratio of precession (~20 kyr) to short (~100 kyr) and long (~400 kyr) eccentricity cycles. This change is theoretically a steady decrease in the precession period due to tidal friction that should increase the ratio of climatic precession to eccentricity cycles (Figure P92). The same effect is seen in obliquity. The actual change in precession, however, may be more complicated due to other factors, especially the changing dynamic

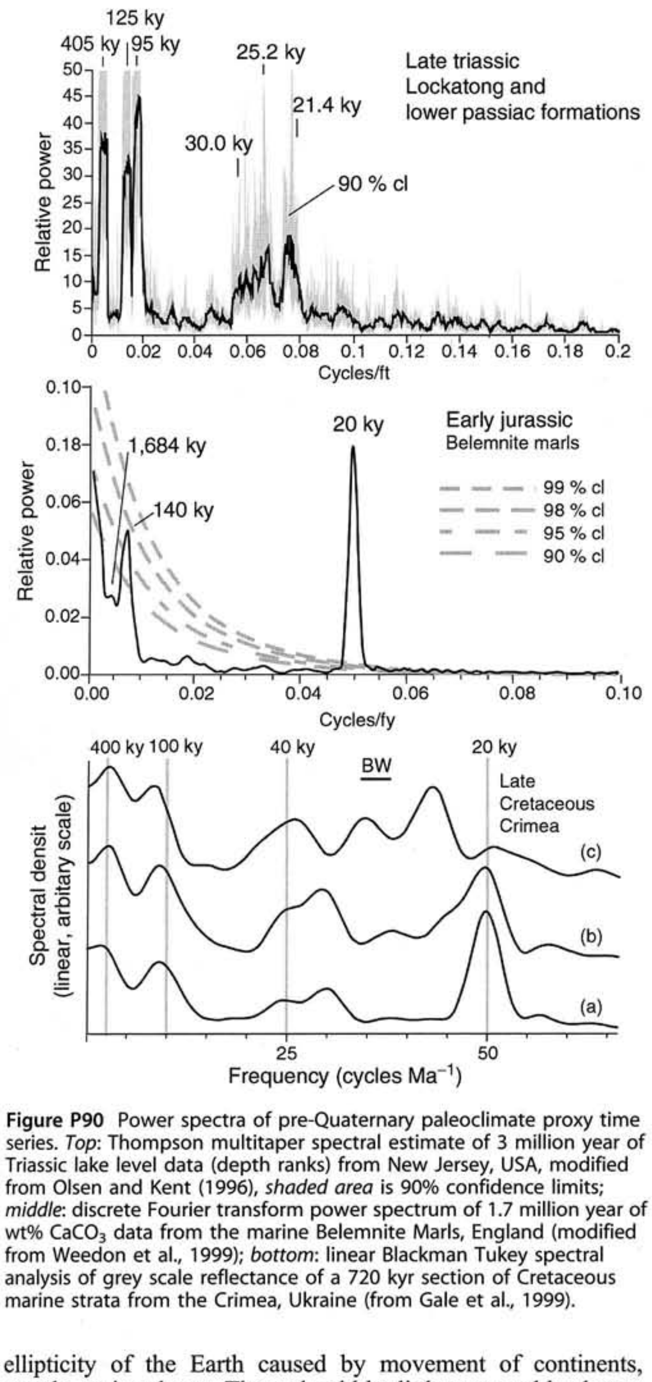

Figure P90 Power spectra of pre-Quaternary paleoclimate proxy time series. *Top*: Thompson multitaper spectral estimate of 3 million year of Triassic lake level data (depth ranks) from New Jersey, USA, modified from Olsen and Kent (1996), *shaded area* is 90% confidence limits; *middle*: discrete Fourier transform power spectrum of 1.7 million year of wt% $CaCO_3$ data from the marine Belemnite Marls, England (modified from Weedon et al., 1999); *bottom*: linear Blackman Tukey spectral analysis of grey scale reflectance of a 720 kyr section of Cretaceous marine strata from the Crimea, Ukraine (from Gale et al., 1999).

ellipticity of the Earth caused by movement of continents, mantle, or ice sheets. There should be little measurable change caused by the chaotic diffusion of the planetary orbits for the typically cited 405 kyr and 100 kyr eccentricity periods, and thus the main observable secular change in orbital frequencies should be in precession.

Many authors have used the canonical 1:5:20 ratio of the shorter to longer cycles as strong evidence of the Milankovitch origin of pre-Quaternary cycles, despite uncertainty in the actual ratio, especially in strata hundreds of millions of years old. In the absence of any other time constraints, these ratios may not be unique (e.g., Latemar controversy, see below). Presuming that the average ratios are broadly consistent with available constraints, and the section covers millions of years, evolutive depth-frequency analysis (as opposed to time-frequency) can reveal shifts in the absolute values of frequencies through a section, while maintaining the ratios of the higher to lower frequencies. Only Milankovitch theory predicts constancy of those frequencies independent of actual accumulation rate. The advantage to this analysis is that the changes in accumulation rate can be derived directly from the spectrogram. At present, only a few sections have been examined this way (e.g., see Olsen and Kent, 1999; Preto et al., 2001; Weedon, 2003).

The interaction of climatic and sedimentological processes should produce a distortion of accumulation rates, resulting in periodograms and time- or depth-frequency spectrograms that are noisy or distorted beyond interpretation. Two techniques, gamma analysis (Kominz and Bond, 1990) and frequency modulation (FM) analysis (Hinnov and Park, 1998) were developed to deal with a situation in which accumulation rate may be a function of Milankovitch cycles themselves. Both involve a version of cycle counting. In gamma analysis, an approximate solution to the relationship between time and facies is found for a succession of sedimentary cycles. Individual facies specific to certain environments are identified within a section and measured in thickness. Assuming that each cycle is of constant duration and each facies is characterized by a specific effective accumulation rate (γ), an approximation of the accumulation rate of each facies can be found by solving a series of simultaneous equations representing the cumulative time of the different facies within each cycle. The fit of these approximations is assessed by an inverse method using the accumulation rates derived from the measured section and Fourier analysis of the resulting time series. If the accumulation rates are identified correctly and the sequence is of Milankovitch origin, the Fourier spectrum should reflect a better fit to the expectations of Milankovitch theory than the original data. Although this method incorrectly assumes a constant duration for the precessional cycles, it might reveal the presence of another cycle to which the section could be tuned, such as the 40 kyr obliquity cycle of relatively constant frequency. This method has been applied to Cambrian marine, and Triassic and Jurassic lacustrine sequences, significantly improving the spectral properties of the data.

FM analysis begins with the identification of the presumed geological expression of precessional (or obliquity) cycles and estimation of the length of each cycle, creating a new time series of depth against cycle thickness. Fourier analysis of this new time series reveals the FM modulating cycles. Since the precession cycle is frequency modulated by the "eccentricity" cycles, FM analysis of a real insolation curve reveals the eccentricity cycles (see Hinnov, 2000). FM analysis of the data curve also has this characteristic shape if it is the result of Milankovitch processes. A tacit assumption of this method is that there is a strong and amplified link between the frequency modulators of accumulation rate and the eccentricity cycles themselves. A major disadvantage to this method is that the higher frequency cycles must be identified, which is nearly impossible in noisy, low amplitude, or clipped records. In addition, the Fourier FM spectral pattern may not be unique to the frequency band characterized by the "usual" Milankovitch frequencies; it may be shared with sub-Milankovitch, yet still quasiperiodic, climatic processes.

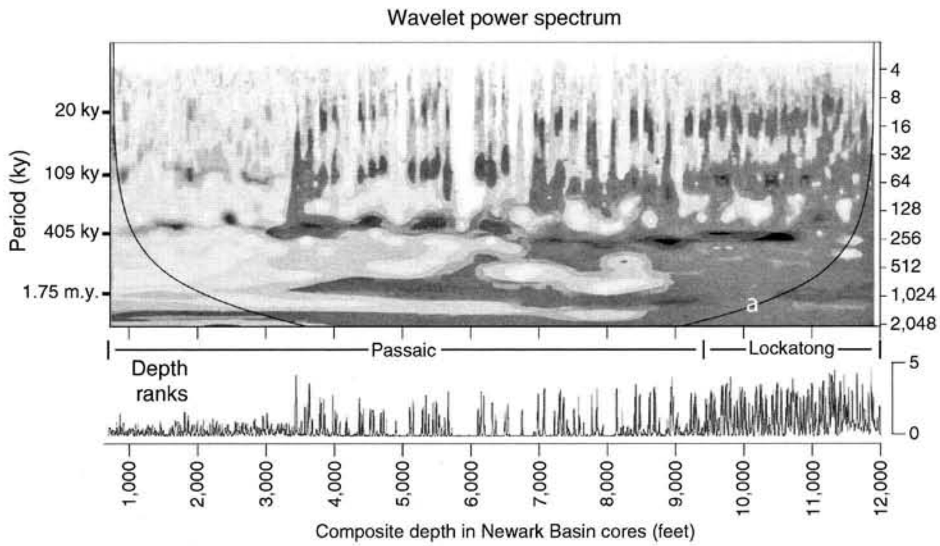

Figure P91 Evolutive spectral analysis of 22 million year of lake level (depth rank) data from the continuously cored Late Triassic age lacustrine Lockatong and Passaic formations of the Newark Rift basin, New Jersey, USA. *Above*: continuous wavelet transform of lake level data (wavelet provided by C. Torrence and G. Compo; *http://paos.colorado.edu/research/wavelets/run* by M. Machlus); *bottom*: depth rank data in depth domain (from Olsen and Kent, 1996).

Proxies

Since climate parameters cannot be measured in sedimentary strata, a reasonably direct recorder of a response to climate change, or climate proxy, is necessary. For Quaternary sequences, a vast array of possible climate proxies can be reasonably calibrated because neither the tectonic plate configuration nor species composition has changed much over the last 2 million years. These proxies include $\delta^{18}O$, a proxy mostly for ice volume (e.g., Hays et al., 1976), eolian dust, a proxy mainly for aridity and wind intensity, and pollen and spores, a reflection of climate-related changes in plant species distributions. Deeper in time these proxies can be affected by diagenesis, lithification, and lack of extant taxa that can be calibrated. Proxies less prone to time-related processes range from sedimentary facies classifications sensitive to water depth (e.g., Olsen, 1986) to geochemical proxies such as $\delta^{13}C$ of organic matter, carbonate sensitive to climate-related oceanographic processes, and oil-shale yield, related to water depth (e.g., Bradley, 1929).

Examples of pre-Quaternary Milankovitch cycles

Neogene

Largely circum-Mediterranean and deep sea core sections are the basis of a high resolution Miocene to Quaternary Milankovitch-cycle-calibrated timescale (Shackleton et al., 1990; Hilgen, 1991b; Hilgen et al., 1995, 1997). The Mediterranean marine sections exhibit the marl-sapropel cyclicity originally described from Mediterranean cores. The largest-scale bundles of cycles visible are matched to the 400 kyr of a precession-dominated isolation curve, in a portion of the section that is already well dated. Progressively smaller bundles are matched to the insolation curve, followed by precession-related individual marl-sapropel cycles (Figure P88). Older sections are then spliced. The hierarchical nature of both the bundling and the insolation curve limits potential miscorrelations. Radiometric dates have been used to test the timescale. The astronomical calibration is so robust that it has allowed for a recalibration of the ^{40}K decay constant, itself (Hilgen et al., 1999) now widely adopted. Hilgen's method has also been extended to non-marine strata, particularly in the Miocene (Aziz et al., 2003).

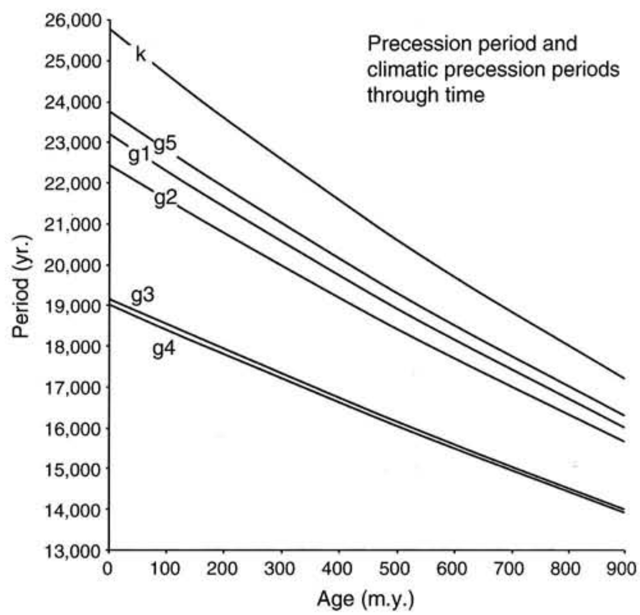

Figure P92 Change in the period of the Earth's axial precession due to tidal friction over the last 900 million years, and the expected changes in climatic precessional cycles. The sum of the frequency of axial precession, *k*, and the various fundamental frequencies of the planets, g1–g5 (only the most important 5 shown here) is equal to the frequency of climatic precession. For the present day, there is a cluster of 3 periods around 23 kyr and another 2 periods around 19 kyr. Derived from Berger et al. (1992).

Shackleton et al. (1999, 2000), Palike et al. (2004), and Billups et al. (2004) have used marine cores showing strong obliquity forcing to produce an astronomical calibration of the Oligocene, Miocene and Neogene. These cores exhibit the usual Milankovitch frequencies and modulation by longer cycles, notably the 1.2 million year cycle of obliquity modulation, and show that the resonance of the orbits of Earth and Mars has not changed state for the last 30 million years.

Paleogene

The description by Bradley (1929) of lacustrine cycles in the Eocene Green River Formation in Colorado and Utah is the classic example of pre-Quaternary Milankovitch cycles. Assuming the relationship between oil shale yield and accumulation rate within each facies to be constant, Bradley used oil shale yield as a proxy for accumulation rate within several sections of a few cycles each. The duration of each cycle was estimated at an average ~21 kyr using the accumulation rates derived from varve calibration. Recently, $^{40}Ar/^{39}Ar$ dates from tuffs within the Green River Formation and cycle counting (without quantitative time-series analysis) have been used to argue that the accumulation rate of the strata was too slow for the individual cycles to average 21 kyr (e.g., Pietras et al., 2003; countered by Machlus et al., 2004, 2008).

Cretaceous

One of the first quantitative applications of the astronomical theory of climate change was by Gilbert (1895) who hypothesized that the marine limestone-shale bedding rhythms of the late Cretaceous of Colorado were of precessional origin. Based on extrapolation from admittedly very limited outcrops, he estimated the duration of the late Cretaceous to be between 20 and 40 million year, favoring 20 million year. Current estimates place the duration of that epoch to be ~34 million year. More recent analysis shows that Gilbert's hypothesis is largely correct and that obliquity and eccentricity cycles are also important (Figure P90). There are many other modern treatments of Cretaceous marine cyclicity (see Hinnov, 2005). Herbert and D'Hondt (1990) used the Milankovitch cyclicity of the latest Cretaceous and earliest Cenozoic (Mastrictian and Danian) cores from the South Atlantic to estimate accumulation rates across the Cretaceous-Tertiary boundary and found an essentially stepwise decrease in accumulation rates consistent with an abrupt boundary event.

Jurassic

Among the first to recognize cyclicity attributable to Milankovitch processes, Schwarzacher (1964) recognized that the Alpine Jurassic carbonate cycles attributed to ~20 kyr precession were bundling into ~100 kyr eccentricity cycles. According to Weedon (2003), the European Tethyian marine sequences are dominated by obliquity-forced cycles in the Hettangian and Sinemurian age parts of the sections, precession in the Pliensbachian (Figure P90), and a mixture of precession and obliquity in the Kimmerigian (see Hinnov, 2005 for additional references). In eastern North America, Olsen et al. (1996) and Whiteside et al. (2007) described lacustrine cyclicity ascribed to precession and eccentricity forcing, and used it to constrain the duration of the Central Atlantic Magmatic Province (~600 kyr), the most geographically-extensive continental flood basalt province on Earth. Olsen et al. (2002) also used the Milankovitch cyclostratigraphy of the latest Triassic and earliest Jurassic to determine the duration of the Triassic-Jurassic boundary events.

Triassic

Schwarzacher (1948, 1954) and Fischer (1964, 1991) recognized a hierarchy of cycles, termed Lofer cycles, within late Triassic age carbonates of the Italian Alps (Norian-Rhaetian), attributing them to the precession and the ~100 and 405 kyr eccentricity cycles (Figure P89). Van Houten (1964) likewise recognized a hierarchy of lake level cycles within the continental late Triassic Newark Supergroup of the Newark rift basin of New York, New Jersey and Pennsylvania using varve calibration and constraints imposed by the duration of the late Triassic itself (Figure P88). This work has been fully supported by later work (e.g., Figure P90), and led to the Newark Basin Coring Project that continuously cored virtually the entire Newark basin sedimentary record (Figure P93). The lacustrine portion of the core record spans 25 million years (Norian-Hettangian) and is characterized by a continuous Milankovitch pattern of lacustrine cycles revealing the full spectrum of precessional and eccentricity frequencies including the longest frequency cycle with periods of 1.75 and 3.5 million year, corresponding to today's 2.4 and 4.8 million year eccentricity cycles (Figure P91). The difference is attributed to chaotic drift in the fundamental orbital frequencies of Earth and Mars (g3 and g4 of Laskar, 1990; Olsen and Kent, 1999). The 405 kyr eccentricity cycle is very clear in this record and provides the basis for an astronomically tuned geomagnetic polarity timescale (Kent and Olsen, 1999, 2000) for the late Triassic that has been recently correlated in detail with Tethyan marine records at the sub-stage level (e.g., Muttoni et al., 2004) (Figure P93).

One of the most contentious debates in pre-Quaternary Milankovitch cyclicity is the Latemar controversy. Middle Triassic age cyclical marine carbonate cycles are well exposed in the northern Italian Alps. Originally, Fischer-plot analysis of this section by Goldhammer et al. (1987) suggested a Milankovitch origin of the cyclicity. Buttressed in their interpretation by Fourier and other numerical analyses, Hinnov and Goldhammer (1991) counted ~600 cycles in ~470 m of section that they attributed to precession cycle forcing of sea level over a period of 12 million year (Hinnov, 2000; Preto et al., 2001). This interpretation is directly challenged by radiometric age data from interbedded and correlative tuffs that imply a duration of 0.5–2 million year for this same interval and by the presence of only two magnetic polarity zones (Brack et al., 1996; Kent et al., 2004). This led to the alternative, perhaps in some ways more interesting, interpretation that what were thought to be precessional cycles are in fact very short, sub-Milankovitch cycles imbedded within much thicker precessional cycles (Kent et al., 2004), highlighting the non-uniqueness of the frequency ratios when order of magnitude differences in the possible timescale are involved.

Paleozoic

There are far fewer convincing examples of Milankovitch cyclicity in Paleozoic records because they tend to be shorter and more poorly temporally constrained (see Hinnov, 2005). Using varves in evaporites, Anderson et al. (1972) calibrated accumulation rates of the Permian Castile Formation of New Mexico and recognized the cycle of climatic precession, sub-Milankovitch cycles that he attributed to sun spot cycles, and other periodicities. Rampino et al. (2000) used evolutive Fourier analysis to determine the duration of Permo-Triassic boundary events.

Carboniferous age, often coal-bearing cycles, termed cyclothems, may have a Milankovitch origin (Fischer, 1986). The Carboniferous was a glacial period and glacio-eustatic

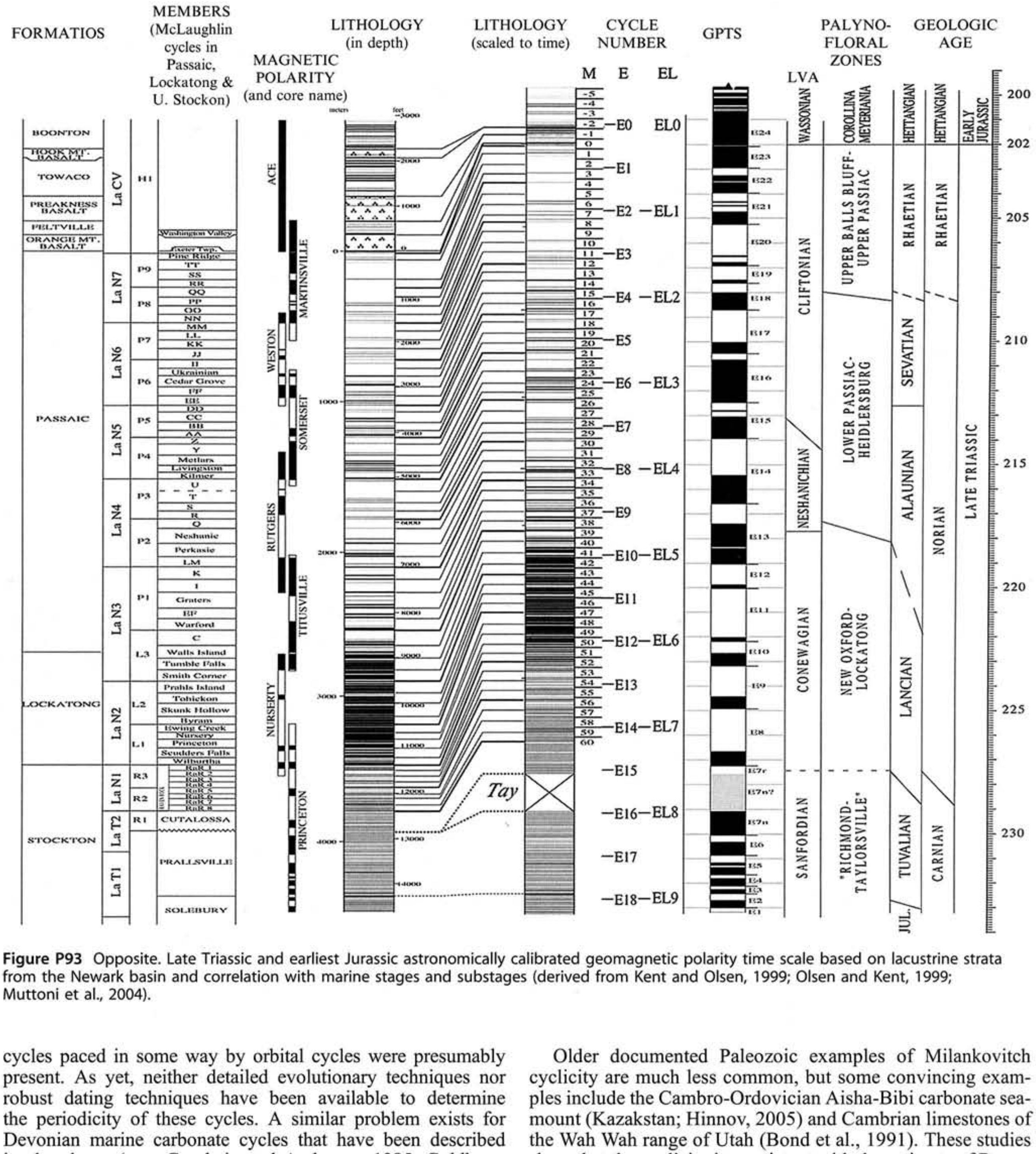

Figure P93 Opposite. Late Triassic and earliest Jurassic astronomically calibrated geomagnetic polarity time scale based on lacustrine strata from the Newark basin and correlation with marine stages and substages (derived from Kent and Olsen, 1999; Olsen and Kent, 1999; Muttoni et al., 2004).

cycles paced in some way by orbital cycles were presumably present. As yet, neither detailed evolutionary techniques nor robust dating techniques have been available to determine the periodicity of these cycles. A similar problem exists for Devonian marine carbonate cycles that have been described in abundance (e.g., Goodwin and Anderson, 1985; Goldhammer et al., 1991; Maynard and Leeder, 1992; Wilkinson et al., 1998; Miller and Eriksson, 1999).

Cyclical lacustrine strata very similar to those present in the Triassic and Jurassic of eastern North America crop out in the Orcadian basin, Scotland (Donovan et al., 1974; Donovan, 1980). Astin (1990) has demonstrated that these strata appear to possess a hierarchy of cycles compatible with a Milankovitch origin.

Older documented Paleozoic examples of Milankovitch cyclicity are much less common, but some convincing examples include the Cambro-Ordovician Aisha-Bibi carbonate seamount (Kazakstan; Hinnov, 2005) and Cambrian limestones of the Wah Wah range of Utah (Bond et al., 1991). These studies show that the cyclicity is consistent with the estimate of Berger et al. (1989) for the Cambrian precessional frequency.

Precambrian

Precambrian examples of Milankovitch forcing are even less well documented. The best-known example is the 2.2 billion year of cyclicity in the Proterozoic Rocknest Formation of the Wopmay Orogen, N.W.T., Canada (Grotzinger, 1986). The sequence consists of asymmetrical carbonate cycles analyzed using Fischer plots. Hofmann et al. (2004) used Markov chain analysis and Fischer plots to examine Archean carbonate cyclicity in the Belingwe Greenstone Belt of Zimbabwe. They pointed out a strong correspondence between the bundling of 7–11 short cycles per long cycle and the predicted ratio by Berger et al. (1989) between precession and short eccentricity cycles.

Challenges

Milankovitch cycles result from the combined gravitational effects of the other bodies in the solar system upon the Earth's spin axis and orbit, and similar effects are thought to be present on other planets (e.g., Kieffer and Zent, 1992; Correia and Laskar, 2001). It is not surprising that orbital cycles have affected the climate and the resulting sedimentary record through Earth's history, and thus the discovery of past Milankovitch cyclicity is less interesting for itself than for its possible uses. Four main challenges facing future work on pre-Quaternary Milankovitch cyclicity can be identified: (a) continued documentation of the orbital cyclicity into older strata with sufficient precession to discriminate deviations from the existing simple models of the secular evolution of the Earth's axial and orbital dynamics, (b) analysis of very long records (10s of millions of years) from various parts of Earth's history to calibrate the chaotic drift in the fundamental frequencies of the solar system (e.g., Olsen and Kent, 1999; Palike et al., 2004) with the ultimate goal of producing insolation curves for any arbitrary time in Earth history, (c) using Milankovitch cycles as a tool for high-resolution correlation and the calibration of other processes in truly ancient sequences, and (d) understanding the mechanisms by which insolation changes result in changes in Earth system processes and the resulting geological record.

Paul E. Olsen and Jessica H. Whiteside

Bibliography

Anderson, R.Y., 1964. Varve calibration of stratification. *Kansas Geological Survey Bulletin* **169**, 1–20.

Anderson, R.Y., and Dean, W.E., 1988. Lacustrine varve formation through time. *Palaeogeogr. Palaeoclimatol. Palaeoecol.*, **62**, 215–235.

Anderson, R.Y., Dean, W.E., Kirkland, D.W., and Snyder, H.I., 1972. Permian Castile varved evaporite sequence, West Texas and New Mexico. *Geol. Soc. Am. Bull.*, **83**, 59–86.

Astin, T.R., 1990. The Devonian lacustrine sediments of Orkney, Scotland; implications for climate cyclicity, basin structure and maturation history. *J. Geol. Soc., London*, **147**, 141–151.

Aziz, A.H., Hilgen, F.J., Wilson, D.S., Krijgsman, W., and Calvo, J.P., 2003. An astronomical polarity timescale for the middle Miocene based on continental sequences. *J. Geophys. Res.*, **108**, 2159

Berger, A., Loutre, M.F., and Dehant, V., 1989. Pre-Quaternary Milankovitch frequencies. *Nature*, **342**, 133.

Berger, A.M., Loutre, M., and Laskar, J., 1992. Stability of the astronomical frequencies over the Earth's history for paleoclimate studies. *Science*, **255**, 260–566.

Billups, K., Palike, H., Channell, J., Zachos, J., and Shackleton, N., 2004. Astronomic calibration of the Late Oligocene through Early Miocene geomagnetic polarity time scale. *Earth Planet. Sci. Lett.*, **224**, 33–44.

Bond, G.C., Kominz, M.A., and Beavan, J., 1991. Evidence for orbital forcing of Middle Cambrian peritidal cycles: Wah Wah Range, south-central Utah. In Watney, L., Franseen, E., Kendall, C., and Ross, W. (eds.), *Sedimentary Modeling: Computer Simulations and Methods for Improved Parameter Definition*. Kansas Geological Survey Bulletin 233, pp. 293–318.

Boss, S.K., and Rasmussen, K.A., 1995. Misuse of Fisher plots as sea-level curves. *Geology*, **23**, 221–224.

Brack, P., Mundil, R., Meier, M., Oberli, F., and Rieber, H., 1996. Biostratigraphic and radiometric age data question the Milankovitch characteristics of the Latemar cycles (Southern Alps, Italy). *Geology*, **24**, 371–375.

Bradley, W.H., 1929. The varves and climate of the Green River epoch. *U.S. Geological Survey Professional Paper*, **158**, 87–110.

Cande, S.C., and Kent, D.V., 1995. Revised calibration of the geomagnetic polarity timescale for the late Cretaceous and Cenozoic. *J. Geophys. Res.*, **100**, 6093–6095.

Correia, A.C., and Laskar, J., 2001. The four final rotation states of Venus. *Nature*, **411**, 767–770.

Donovan, R.N., 1980. The lacustrine cycles, fish ecology and stratigraphic zonation in the middle Devonian of Caithness. *Scott. J. Geol.*, **16**, 35–50.

Donovan, R.N., Foster, R.J., and Westoll, T.S., 1974. A stratigraphical revision of the Old Red Sandstone of northeastern Caithness. *Trans. R. Soc. Edinb.*, **69**, 171–205.

Fischer, A.G., 1964. The Lofer cyclothems of the Alpine Triassic. *Kansas Geological Survey Bulletin* **169**, 107–149.

Fischer, A.G., 1986. Climatic Rhythms Recorded in Strata. *Annu. Rev. Earth Planet. Sci.*, **14**, 351–376.

Fischer, A.G., 1991. Orbital cyclicity in Mesozoic strata. In Einsele, G., Ricken, W., and Seilacher, A. (eds.), *Cycles and Events in Stratigraphy.* Berlin: Springer, pp. 48–62.

Fischer, A.G., Herbert, T.D., Napoleone, G., Premoli Silva, I., and Ripepe, M., 1991. Albian pelagic rhythms (Piobbico Core). *J. Sediment. Res.*, **61**, 1164–1172.

Gale, A.S., Young, J.R., Shackleton, N.J., Crowhurst, S.J., and Wray, D.S., 1999. Orbital tuning of Cenomanian marly chalk successions: Towards a Milankovitch time-scale for the Late Cretaceous. *Philos. Trans. R. Soc. London, Math. Phys. Eng. Sci.*, **357**, 1815–1829.

Gilbert, G.K., 1895. Sedimentary measurement of Cretaceous time. *J. Geol.*, **3**, 121–127.

Goldhammer, R.K., Dunn, P.A., and Hardie, L.A., 1987. High frequency glacio-eustatic oscillations with Milankovitch characteristics recorded in northern Italy. *Am. J. Sci.*, **287**, 853–892.

Goldhammer, R.K., Oswald, E.J., and Dunn, P.A., 1991. Hierarchy of stratigraphic forcing – example from Middle Pennsylvanian shelf carbonates of the Paradox basin. In Franseen, E.K., Watney, W.L., Kendall, C.G. St. C., and Ross, W. (eds.), *Sedimentary Modeling: Computer Simulations and Methods for Improved Parameter Definition*. Kansas Geological Survey Bulletin 233, pp. 361–413.

Goodwin, P.W., and Anderson, E.J., 1985. Punctuated Aggradational Cycles: A General Model of Stratigraphic Accumulation. *J. Geol.*, **93**, 515–534.

Grotzinger, J.P., 1986. Upward shallowing platform cycles: A response to 2.2 billion years of low-amplitude, high-frequency (Milankovitch band) sea level oscillations. *Paleoceanography*, **1**, 403–416.

Hays, J.D., Imbrie, J., and Shackleton, N.J., 1976. Variations in the Earth's orbit: Pacemaker of the ice ages. *Science*, **194**, 1131–1133.

Herbert, T.D., and D'Hondt, S.L., 1990. Precessional climate cyclicity in Late Cretaceous-Early Tertiary marine sediments: A high resolution chronometer of Cretaceous-Tertiary boundary events. *Earth Planet. Sci. Lett.*, **99**, 263–275.

Hilgen, F.J., 1991a. Astronomical calibration of Gauss to Matuyama sapropels in the Mediterranean and implications for the Geomagnetic Polarity Scale. *Earth Planet. Sci. Lett.*, **104**, 226–244.

Hilgen, F.J., 1991b. Extension of the astronomically calibrated (polarity) timescale to the Miocene/Pliocene boundary. *Earth Planet. Sci. Lett.*, **107**, 349–368.

Hilgen, F.J., Krijgsman, W., Langereis, C.G., Lourens, L.J., Santarelli, A., and Zachariasse, W.J., 1995. Extending the astronomical (polarity) timescale into the Miocene. *Earth Planet. Sci. Lett.*, **136**, 495.

Hilgen, F.J., Krijgsman, W., Langereis, C.G., and Lourens, L.J., 1997. Breakthrough made in dating of the geological record. *Eos*, **78**, 285, 288–289.

Hilgen, F.J., Abdul Aziz, H., Krijgsman, W., Langereis, C.G., Lourens, L.J., Meulenkamp, J.E., Raffi, I., Steenbrink, J., Turco, E., and van Vugt, N., 1999. Present status of the astronomical (polarity) time-scale for the Mediterranean Late Neogene. *Philos. Trans. R. Soc. London* (series A), **357**, 1931–1947.

Hinnov, L.A., 2000. New perspectives on orbitally forced stratigraphy. *Annu. Rev. Earth Planet. Sci.*, **28**, 419–475.

Hinnov, L.A., 2005. Astronomical signals from Pre-Cenozoic eras. In Berger, A., and Ercegovac, M. (eds.), *Milutin Milankovitch 125th*

Anniversary Symposium: Paleoclimate and the Earth Climate System, Proceedings of the Serbian Academy of Sciences and Arts, Serbia. Belgrade,

Hinnov, L.A., and Goldhammer, R.K., 1991. Spectral analysis of the Middle Triassic Latemar Limestone. *J. Sediment. Petrol.*, **61**, 1173–1193.

Hinnov, L.A., and Park, J., 1998. Detection of astronomical cycles in the sedimentary record by frequency modulation (FM) analysis. *J. Geophys. Res.*, **68**, 524–539.

Hofmann, A., Dirks, P.H.G.M., and Jelsma, H.A., 2004. Shallowing-upward carbonate cycles in the Belingwe Greenstone Belt, Zimbabwe: A record of Archean sea-level oscillations. *J. Sediment. Res.*, **74**, 64–81.

Kent, D.V., and Olsen, P.E., 1999. Astronomically tuned geomagnetic polarity timescale for the Late Triassic. *J. Geophys. Res.*, **104**, 12831–12841.

Kent, D.V., and Olsen, P.E., 2000. Implications of a new astronomical time scale for the Late Triassic. In Bachmann, G., and Lerche, I. (eds.), *Epicontinental Triassic*, vol 3, Zentralblatt fur Geologie und Palaontologie, VIII, pp. 1463–1474.

Kent, D.V., Muttoni, G., and Brack, P., 2004. Magnetostratigraphic confirmation of a much faster tempo for sea-level change for the Middle Triassic Latemar platform carbonates. *Earth Planet. Sci. Lett.*, **228**, 369–377.

Kieffer, H.H., and Zent, A.P., 1992. Quasi-periodic climate change on Mars. In Kieffer, H.H., Jakosky, B.M., Snyder, C.W., and Matthews, M.S. (eds.), *Mars*, Space Science Series. Tucson, AZ: University of Arizona Press, pp. 1180–1218.

Kominz, M.A., and Bond, G.C., 1990. A new method of testing periodicity in cyclic sediment: Application to the Newark Supergroup. *Earth Planet. Sci. Lett.*, **98**, 233–244.

Laskar, J., 1990. The chaotic motion of the solar system: A numerical estimate of the size of the chaotic zones. *Icarus*, **88**, 266–291.

Laskar, J., 1999. The limits of Earth orbital calculations for geological time-scale use. *Philos. Trans. R. Soc. London, A*, **357**, 1735–1759.

Laskar, J., Joutel, F., and Boudin, F., 1993. Orbital, precessional, and insolation quantities for the Earth from -20 myr to +10 myr. *Astron. Astrophys.*, **270**, 522–533.

Laskar, J., Robutel, P., Joutel, F., Gastineau, M., Correia, A.C.M., and Levrard, B., 2004. A long term numerical solution for the insolation quantities of the Earth. *Astron. Astrophys.*, **428**, 261–285.

Lowrie, W., and Kent, D.V., 2004. Geomagnetic polarity timescales and reversal frequency regimes. In Channell, J.E.T., Kent, D.V., Lowrie, W., and Meert, J. (eds.), *Timescales of the Paleomagnetic Field, AGU Geophysical Monograph 145.* Washington, DC: American Geophysical Union, pp. 117–129.

Machlus, M., Hemming, S.R., Olsen, P.E., and Christie-Blick, N., 2004. Eocene calibration of geomagnetic polarity timescale reevaluated: Evidence from the Green River Formation of Wyoming. *Geology*, **32**, 137–140.

Machlus, M., Olsen, P.E., Christie-Blick, N., and Hemming, S.R., 2008, Spectral Analysis of the Lower Eocene Wilkins Peak Member, Green River Formation, Wyoming: Support for Milankovitch Cyclicity. *Earth Planet. Sci. Lett.*, **286**, 64–75.

Maynard, J.R., and Leeder, M.R., 1992. On the periodicity and magnitude of Late Carboniferous glacio-eustatic sea-level changes. *J. Geol. Soc.*, **149**, 303–311.

Miller, D.J., and Eriksson, K.A., 1999. Linked sequence development and global climate change: The upper Mississippian record in the Appalachian basin. *Geology*, **27**, 35–38.

Miller, K.G., Fairbanks, R.G., and Mountain, G.S., 1987. Tertiary oxygen isotope synthesis, sea level history, and continental margin erosion. *Paleoceanography*, **2**, 1–19.

Muller, R., and MacDonald, G., 2000. *Ice Ages and Astronomical Causes: Data, Spectral Analysis, and Mechanisms.* London: Springer-Praxis, 318pp.

Muttoni, G., Kent, D.V., Olsen, P.E., DiStefano, P., Lowrie, W., Bernasconi, S., and Hernandez, F.M., 2004. Tethyan magnetostratigraphy from Pizzi Mondello (Sicily) and correlation to the Late Triassic Newark astrochronological polarity time scale. *Geol. Soc. Am. Bull.*, **116**, 1043–1058.

Olsen, P.E., 1986. A 40-million-year lake record of early Mesozoic climatic forcing. *Science*, **234**, 842–848.

Olsen, P.E., and Kent, D.V., 1996. Milankovitch climate forcing in the tropics of Pangea during the Late Triassic. *Palaeogeogr. Palaeoclimatol. Palaeoecol.*, **122**, 1–26.

Olsen, P.E., and Kent, D.V., 1999. Long-period Milankovitch cycles from the Late Triassic and Early Jurassic of eastern North America and their implications for the calibration of the early Mesozoic time scale and the long-term behavior of the planets. *Philos. Trans. R. Soc. London* (series A), **357**, 1761–1787.

Olsen, P.E., Schlische, R.W., and Fedosh, M.S., 1996. 580 ky duration of the Early Jurassic flood basalt event in eastern North America estimated using Milankovitch cyclostratigraphy. In Morales, M. (ed.), *The Continental Jurassic.* Flagstaff, AZ: Museum of Northern Arizona. Museum of Northern Arizona Bulletin 60, pp. 11–22.

Olsen, P.E., Kent, D.V., Sues, H.-D., Koeberl, C., Huber, H., Montanari, A., Rainforth, E.C., Fowell, S.J., Szajna, M.J., and Hartline, B.W., 2002. Ascent of dinosaurs linked to an iridium anomaly at the Triassic-Jurassic boundary. *Science*, **296**, 1305–1307.

Palike, H., Laskar, J., and Shackleton, N.J., 2004. Geologic constraints on the chaotic diffusion of the solar system. *Geology*, **32**, 929–932.

Pietras, J.T., Carroll, A.R., Singer, B.S., and Smith, M.E., 2003. 10 k.y. depositional cyclicity in the early Eocene: Stratigraphic and 40Ar/39Ar evidence from the lacustrine Green River Formation. *Geology*, **31**, 593–596.

Preto, N., Hinnov, L.A., Hardie, L.A., and De Zanche, V., 2001. A Middle Triassic orbital signal recorded in the shallow marine Latemar carbonate buildup (Dolomites, Italy). *Geology*, **29**, 1123–1128.

Rampino, M.R., Prokoph, A., and Adler, A., 2000. Tempo of the end-Permian event: High-resolution cyclostratigraphy at the Permian-Triassic boundary. *Geology*, **28**, 643–646.

Sadler, P.M., Osleger, D.A., and Montañez, I.P., 1993. On the labelling, length and objective basis of Fischer plots. *J. Sediment. Petrol.*, **63**, 360–368.

Schwarzacher, W., 1948. Sedimentpetrographische Untersuchungen kalkalpiner Gesteine; hallstaetterkalke von Hallstatt und Ischl. *Jahrbuch der Geologischen Bundesanstalt Wien*, **91**, 1–48.

Schwarzacher, W., 1954. Die Grossrhythmik des Dachsteinkalkes von Lofer. *Tschermak's Mineralogische und Petrographische Meitteilungen*, **4**(1–4), 44–54.

Schwarzacher, W., 1964. An application of statistical time-series analysis of a limestone/shale sequence. *J. Geol.*, **72**, 195–213.

Schwarzacher, W., 1993. Milankovitch cycles in the pre-Pleistocene stratigraphic record; a review. In Hailwood, E.A., and Kidd, R.B. (eds.), *High Resolution Stratigraphy.* Geological Society Special Publications 70, pp. 187–194.

Shackleton, N.J., Berger, A., and Peltier, W.R., 1990. An alternative astronomical calibration of the lower Pleistocene timescale based on ODP Site 677. *Trans. R. Soc. Edinb. Earth Sci.*, **81**, 251.

Shackleton, N.J., Crowhurst, S.J., Weedon, G., and Laskar, L., 1999. Astronomical calibration of Oligocene-Miocene time. *R. Soc. London, Philos. Trans. series A*, **357**, 1909–1927.

Shackleton, N.J., Hall, M.A., Raffi, I., Tauxe, L., and Zachos, J., 2000. Astronomical calibration age for the Oligocene-Miocene boundary. *Geology*, **28**, 447–450.

Van Houten, F.B., 1964. Cyclic lacustrine sedimentation, Upper Triassic Lockatong Formation, central New Jersey and adjacent Pennsylvania. In Mermaid, O.F. (ed.), *Symposium on Cyclic Sedimentation.* Kansas Geological Survey Bulletin 169, 497–531.

Weedon, G.P., 1993. The recognition and stratigraphic implications of orbital-forcing of climate and sedimentary cycles. In Wright, V.P. (ed.), *Sedimentology Review/1.* Oxford, UK: Blackwell Scientific Publications, pp.31–50.

Weedon, G.P., 2003. *Time-series Analysis and Cyclostratigraphy-Examining Stratigraphic Records of Environmental Cycles.* Cambridge, UK: Cambridge University Press, 259pp.

Weedon, G.P., Jenkyns, H.C., Coe, A.L., and Hesselbo, S.P., 1999. Astronomical calibration of the Jurassic time-scale from cyclostratigraphy in British mudrock formations. *Philos. Trans.: Math. Phys. Eng. Sci.*, **357**, 1787–1813.

Whiteside, J.H., Olsen, P.E., Kent, D.V., Fowell, S.J., and Et-Touhami, M., 2007. Synchrony between the CAMP and the Triassic-Jurassic mass-extinction event? *Palaeogeogr. Palaeoclimatol. Palaeoecol.*, **244**, 345–367.

Wilkinson, B.H., Diedrich, N.W., Drummond, C.N., and Rothman, E.D., 1998. Michigan hockey, meteoric precipitation, and carbonate accumulation on peritidal carbonate platforms. *Bulletin of the Geological Society of America*, **110**, 1075–1093.

Cross-references

Astronomical Theory of Climate Change
Atmospheric Evolution, Mars
Cyclic Sedimentation (cyclothems)
Dating, Radiometric Methods
Eccentricity
Monsoons, Pre-Quaternary
Monsoons, Quaternary
Obliquity
Oxygen Isotopes
Precession, Climatic
Quaternary Climate Transitions and Cycles
SPECMAP
Time-Series Analysis of Paleoclimate Data
Varved Sediments